Energy and AI 17 (2024) 100415

Contents lists available at ScienceDirect

Energy and AI

journal homepage: www.sciencedirect.com/journal/energy-and-ai

Machine learning modeling for fuel cell-battery hybrid power system dynamics in a Toyota Mirai 2 vehicle under various drive cycles

Adithya Legala [a,b], Matthew Kubesh [a], Venkata Rajesh Chundru [a], Graham Conway [a,*], Xianguo Li [b,*]

[a] Southwest Research Institute, San Antonio, TX, USA
[b] Department of Mechanical and Mechatronics Engineering, University of Waterloo, Waterloo, Ontario, Canada

HIGHLIGHTS

- Measured fuel cell-battery hybrid power system dynamics in a Toyota Mirai 2 vehicle.
- Data taken from Mirai CAN bus in chassis dynamometer tests for various drive cycles.
- Designed machine learning architecutre to model real-time power dynamic attributes.
- Included dynamic attriburtes of both fuel cell and lithium-ion battery pack.
- Found the developed machine learning model accurately predict real-time dynamics.

GRAPHICAL ABSTRACT

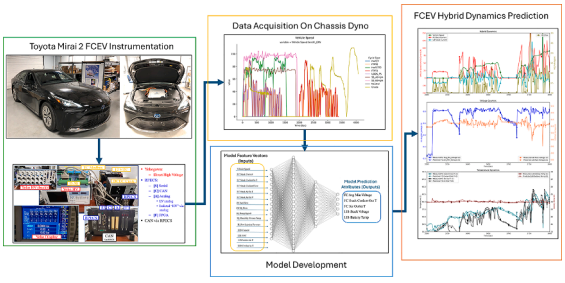

ARTICLE INFO

Keywords:
Artificial neural network (ANN)
Proton exchange membrane fuel cell (PEMFC)
Fuel cell electric vehicle (FCEV)
Fuel cell-battery electric-electric hybrid power system
Data-based models
Lithium-ion battery (LiB)

ABSTRACT

Electrification is considered essential for the decarbonization of mobility sector, and understanding and modeling the complex behavior of modern fuel cell-battery electric-electric hybrid power systems is challenging, especially for product development and diagnostics requiring quick turnaround and fast computation. In this study, a novel modeling approach is developed, utilizing supervised machine learning algorithms, to replicate the dynamic characteristics of the fuel cell-battery hybrid power system in a 2021 Toyota Mirai 2nd generation (Mirai 2) vehicle under various drive cycles. The entire data for this study is collected by instrumenting the Mirai vehicle with in-house data acquisition devices and tapping into the Mirai controller area network bus during chassis dynamometer tests. A multi-input - multi-output, feed-forward artificial neural network architecture is designed to predict not only the fuel cell attributes, such as average minimum cell voltage, coolant and cathode air outlet temperatures, but also the battery hybrid system attributes, including lithium-ion battery pack voltage and temperature with the help of 15 system operating parameters. Over 21,0000 data points on various drive cycles having combinations of transient and near steady-state driving conditions are collected, out of which around 15,000 points are used for training the network and 6,000 for the evaluation of the model performance. Various data filtration techniques and neural network calibration processes are explored to condition the data and understand the impact on model performance. The calibrated neural network accurately predicts the hybrid power system dynamics with an R-squared value greater than 0.98, demonstrating the potential of machine learning algorithms for system development and diagnostics.

* Corresponding authors.
E-mail addresses: graham.conway@swri.org (G. Conway), xianguo.li@uwaterloo.ca (X. Li).

https://doi.org/10.1016/j.egyai.2024.100415

Available online 13 August 2024

1. Introduction

Transport sector, including land transportation, surface ships, and aviation, contributes to about one-third of the world's anthropogenic greenhouse gas emissions [1,2] and is recognized to be the most difficult to decarbonize due to its mobile, transient, and distributed nature and variable drive/load conditions as well as extensive infrastructure spread over large areas [3,4]. Hence, electrification is essential for the decarbonization of the mobility sector, mainly through the development and deployment of battery electric, fuel cell electric, and fuel cell-battery electric-electric hybrid power systems – hybridization resolves range anxiety, offers fast refueling and fast load response, and alleviates the excessive degradation arising from variable load operations [5–7]. As a result, almost all fuel cell electric vehicles (FCEVs) are actually powered by fuel cell-battery hybrid systems, and the development and deployment of FCEVs will revolutionize sustainable transportation and address critical environmental challenges [8,9].

The 2021 Toyota Mirai 2nd generation (hence often referred to as Mirai 2) marks a significant milestone in the development and commercialization of FCEVs, and its complex operational strategy, hybrid energy management, is regarded as a benchmark in the automotive industry [10,11]. It is challenging to develop models of such complex fuel cell systems that can run in real-time for diagnostics and system development using traditional empirical or physics-based models, especially if the system attributes and material properties are not available [12–15]. The dynamic nature of power demands and the interactions between the fuel cell and battery during various driving conditions require sophisticated modeling techniques to capture transient behaviors accurately across the drive cycle [16–19]. Components such as the fuel cell stack exhibit non-linear behaviors due to electrochemical reactions, temperature variations, and humidity levels, and these nonlinearities require advanced mathematical modeling and computational approaches [20–22]. The fuel cell's core involves electrochemical reactions influenced by numerous factors, including catalyst properties, membrane conductivity, gas diffusion layers, liquid flow within the fuel cell, and the associated manifolds, which are critical for performance prediction [23–25] Considering the onboard diagnostics/prognostics and product development applications for an FCEV hybrid power system, a computationally fast and accurate model is essential to predict system outputs such as fuel cell voltage, fuel cell coolant out temperature, fuel cell air outlet temperature, battery pack voltage, and battery temperature over various driving conditions.

Most of the existing literature on fuel cell-battery hybrid modeling and FCEV energy dynamics focuses on a cell level, small stacks, or a virtual environment; it is very limited for the development of models from a vehicle point of view and experimentally validating them on a drive cycle with the vehicle's data acquisition system and controller area network (CAN) bus signals. Mauro [26] developed an empirical powertrain model to understand and optimize the energy management in the Toyota Mirai based on the CAN data acquired from the vehicle while operating at Argonne National Laboratory. In this study, Mauro utilized multiple curve fitting models to somewhat replicate the behavior of fuel cell battery voltage dynamics but could not comprehend the thermal behavior. Such empirical models can help simulate the energy management strategy. Still, they cannot be used for diagnostics or system development as they lack a correlation with reactant pressures and flow rates. Venkata [27] has developed a fuel cell hybrid model to downsize the fuel cell stack and analyzed the behavior on various drive cycles in a MATLAB – SIMULINK-based virtual environment; however, this lacks any experimental validation and consideration of thermal constraints. Markus [28] has experimentally investigated the aspect of reverse engineering the Toyota Mirai vehicle by collecting the data and investigating the behavior of the hybrid system over different driving profiles, providing valuable insights; however, the study lacked the model development aspect that can replicate the behavior in a virtual environment. Tsuyoshi [29] published their research on developing a physics-based fuel cell control system for Mirai vehicles to address vehicle operation at sub-zero temperature conditions. This study considers the thermal aspects, water balance of the fuel cell hybrid system, and operational strategy but misses the role of battery dynamics, and most of the physical parameters needed for the model are not disclosed. Hasegawa [17] has comprehensively modeled the dynamics of the Mirai fuel cell system using the physics-based approach and considered all the reactant flow parameters and associated thermal attributes. However, such models cannot parallelly accommodate battery dynamics and will need another similar model to simulate hybrid dynamics.

The objective of the present study is therefore to develop an accurate and computationally fast predictive model for fuel cell-battery electric-electric hybrid power systems for vehicles, that can be used for the development and diagnostics of such hybrid systems in real time. The dynamic behavior of the hybrid power system is measured when the FCEV, Toyota Mirai 2, is on chassis dynamometer tests under various drive cycles covering a broad spectrum of vehicle operating conditions. Then machine learning algorithms, such as neural networks, are developed based on these vehicle test data to achieve a rapid computational model with accurate prediction of the critical outputs of the fuel cell and battery dynamics over a drive cycle. Correlations between the hybrid system operating parameters are identified, and the appropriate feature vectors and prediction attributes are developed. The machine learning model is trained on data obtained from various drive cycles having combinations of near-steady-state and transient driving conditions, and their prediction accuracy is evaluated. The developed machine learning model is accurate and computationally fast to be useful for real-time diagnostics or system development.

Table 1
Specification for the 2021 Mirai 2nd generation fuel cell electric vehicle (FCEV) tested in the present study.

Attribute	*Value*	
Range	402 mi (647 km)	Vehicle specification
Fuel economy - city/ highway/combined	76/71/74 MPGe	
0 – 60 mph	9.0 s	
Maximum speed	108 mph (175 km/h)	
Fuel	Hydrogen (H_2)	
Purity of H_2	99.97 %	
Storage	3 x type four hydrogen tanks	
Tank capacity	5.6 kg (12.3 lbs)	
Power plant	Fuel-cell electric	Fuel cell (FC) stack specification
Number of fuel cells	330	
Specific power density	5.4 kW/l	
Power	128 kW (172 bhp)	
Aspiration	Inlet air compressor	
Motor location	Rear wheel drive	Transmission specification
Power	136 kW (182 hp)	
Torque	300 N-m (221 lb-ft)	
Battery cells	84	Lithium battery (LIB) pack specification
Nominal voltage	310.8 V	
Energy capacity	1.24 kWh / 4.0 Ah	
Peak output	31.5 kW x 10 s	
Battery pack mass	44.6 kg	
Energy density	27.6 Wh/kg	

2. Data acquisition procedure

The 2021 Toyota Mirai XLE, with the specifications listed in Table 1, was procured and instrumented with sensors to measure voltages, current, power, pressure, flow, temperature, and the OEM CAN signals. All signals were captured on state-of-the-art in-house data acquisition systems, and high-speed CAN signals from the non-OBD (on-board diagnostics) proprietary bus were reverse-engineered using SwRI intellectual property. A Yokogawa power analyzer was used to measure AC, DC, and power factor signals in the fuel cell, inverter, and motor. Wire routing had to be optimized to minimize electromagnetic

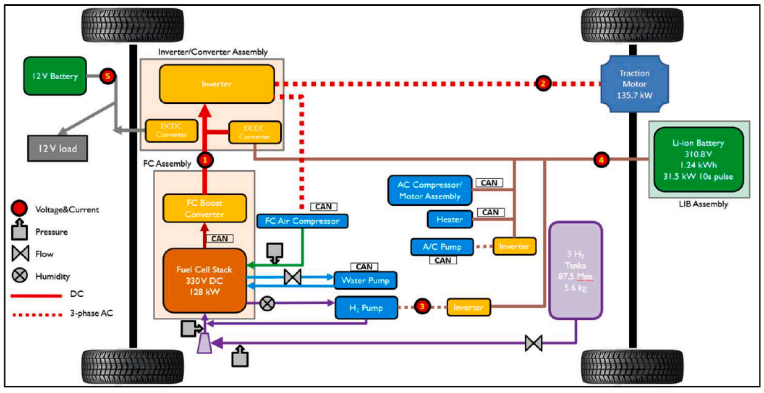

(A)

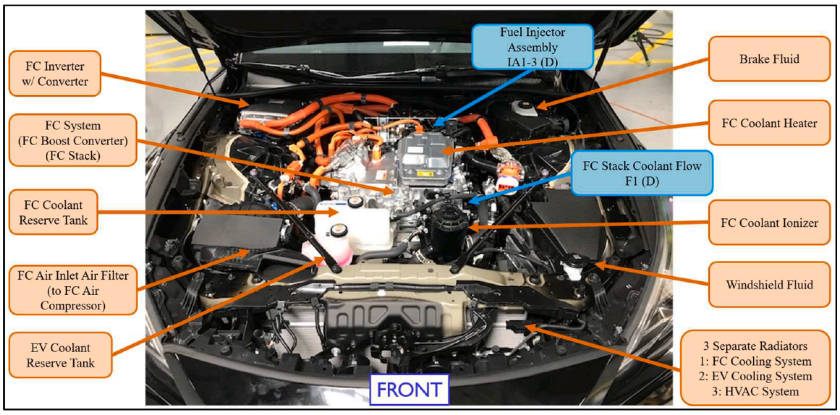

(B)

Fig. 1. 2021 Toyota Mirai 2 fuel cell electric vehicle. (A) Schematic of, and (B) the actual layout (under the hood) of, the fuel cell-lithium-ion battery hybrid powertrain system.

interference between high-power motor power signals and data acquisition signals. The test matrix and vehicle instrumentation were focused on acquiring the vehicle data on relevant drive cycles using a chassis dynamometer. The driving tests extracted data on the hybrid operation of the fuel cell and battery during transient and near-steady-state maneuvers as specified by the driving cycles. Test data was used to evaluate and understand the behavior of fuel cell stack, high-voltage systems, lithium batteries, and drive motors.

Fig. 1 illustrates the 2021 Mirai 2 FCEV powertrain architecture and the systems in the fuel cell (FC) compartment under the front hood. The air and hydrogen react in the FC stack to generate electrical potential, and the FC boost converter then steps up the FC stack voltage. The FC inverter with converter assembly receives power from the FC boost converter or the lithium-ion battery (LIB), depending on the direction of the demand. When the traction drive motor demands power, the inverter inverts the power from DC to 3-phase AC and sends power to the drive motor. When the regenerative braking is active, the converter converts the power from 3-phase AC to DC and sends power to the LIB to increase its state of charge (SOC). The LIB pack receives a charge from the FC boost converter when the SOC is low enough to accept a charge and when there is no drive motor demand on the LIB.

The chassis dynamometer tests were performed on a Horiba 48-inch single-roll chassis dynamometer. Chassis dynamometer coefficients and equivalent test weights were taken from the Environmental Protection Agency's (EPA) test car list. Dyno set coefficients were determined using test procedure SAE J2264 [30]. The vehicle was operated in dyno mode during all testing phases; following J2572 [31], the car was driven over the EPA Urban Dynamometer Driving Schedule (UDDS) [32] and the Highway Fuel Economy Test (HwFET) [32]. Vehicle data was acquired on UDDS, Federal Test Procedure (FTP) [32], Highway Fuel Economy Test (HwFET), Neutral Cycle (In neutral/idle), and Gradient Cycle (Grade Testing Cycle). The gradient cycle is a non-standard in-house cycle designed to record operational data by pushing the vehicle to maximum operating conditions. The Mirai vehicle was repeatedly operated at full pedal on the dyno at different loads and speeds during the gradient cycle until the vehicle changed operational strategies and finally hit a thermal derate.

3. Vehicle data

The operating parameters for the vehicle's fuel cell and battery system, such as stack current, voltage, reactant flow rates, reactant pressures, coolant temperatures, air temperatures, and vehicle speed, are acquired during the experimentation and illustrated using pair plots as shown in Figs. 2, 3, and 4. A total of over 21,000 data points are collected for the vehicle running on various drive cycles, including

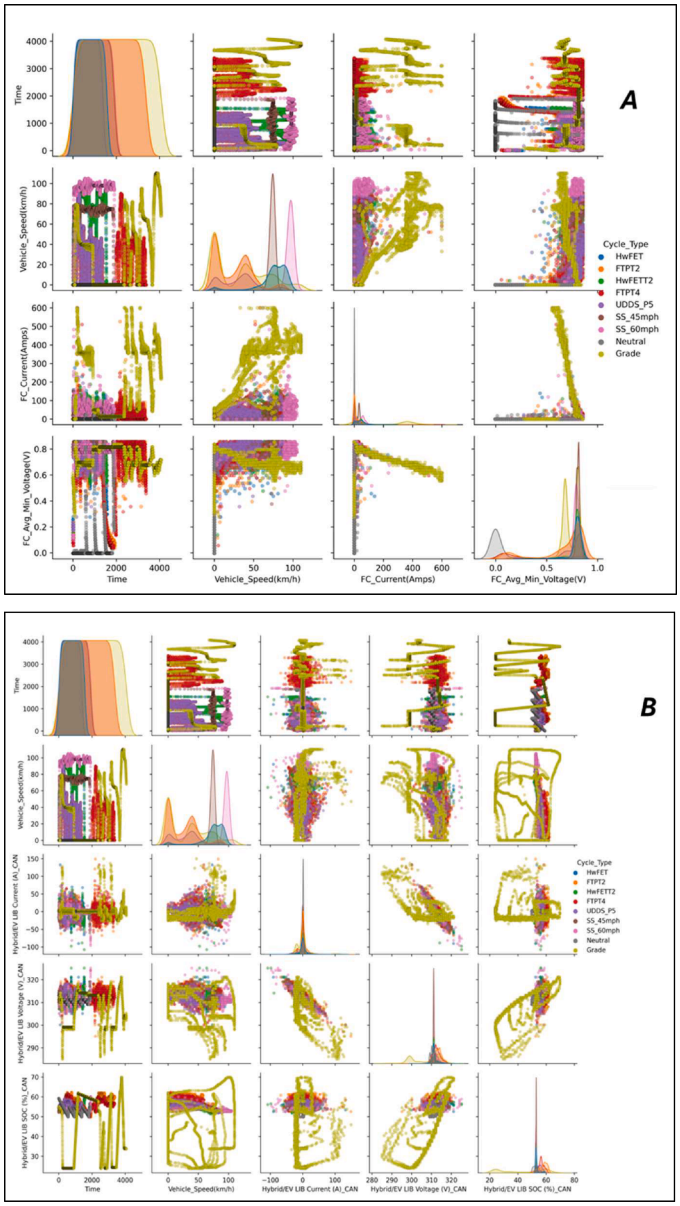

Fig. 2. The electrical attributes of the 2021 Toyota Mirai 2 fuel cell electric vehicle under various loading conditions, as represented by the data acquired in this study: (A) Fuel cell (FC) stack; (B) Lithium-ion battery (LiB) Pack.

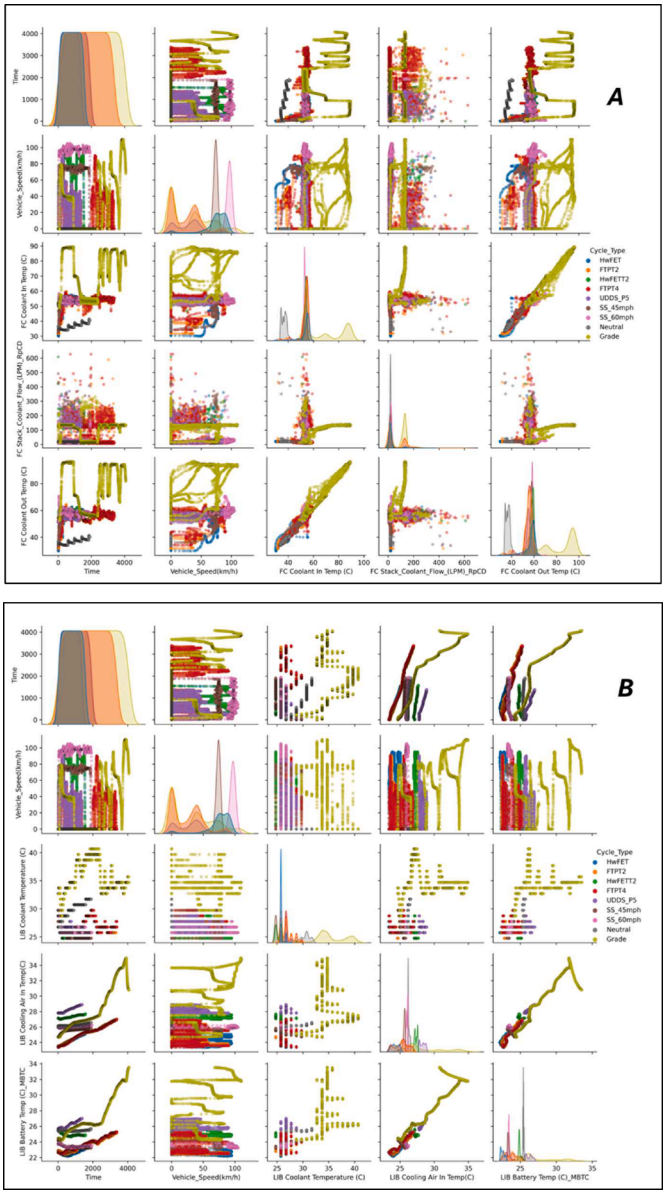

Fig. 3. The thermal attributes of the 2021 Toyota Mirai 2 fuel cell electric vehicle under various loading conditions, as represented by the data acquired in this study: (A) Fuel cell (FC) stack; (B) Lithium-ion battery (LiB) Pack.

transient and near-steady-state driving conditions. The Mirai vehicle, similar to other light-duty vehicles, predominantly operates by utilizing less than 50 kW of power and maintains the fuel cell stack coolant temperature around 55°C to 65°C during normal driving conditions, be standard or near steady-state drive cycles. The battery pack is maintained around 25°C to 30°C and at a state of charge (SOC) between 50 % to 60 % when operated on standard drive cycles. However, during peak load conditions, i.e., during the gradient cycle, the fuel cell can produce close to 110–120 kW. The fuel cell coolant temperature rose close to 95°C during the peak load, and exceeding this temperature resulted in a thermal derate condition to protect the fuel cell system; during these high loads, the battery pack's SOC also dropped to 20 %, and the battery temperature rose to 35°C. Fig. 2 illustrates the correlation between the vehicle speed, fuel cell, and lithium battery operating parameters during various drive cycles; here, besides standard drive cycles, 'SS_45' and 'SS_60' refer to near-steady-state driving around 45 and 60 miles per hour, 'Neutral' refers to the vehicle in neutral/idle condition after running for a while. It can be noted from Fig. 2 that a wide range of vehicle speeds from idle to 100 km/h are covered under the test matrix. The gradient cycle pushes the fuel cell into an unusually high load condition, facilitating data acquisition in extreme conditions to cover the entire spectrum of the powertrain operation.

Fig. 3 illustrates the thermal management system behavior of the fuel cell and battery; the data is very transient as the coolant and reactant flow attributes directly correlate to the vehicle's power demand, i.e., load on the fuel cell and battery. Neutral and gradient cycles are the two outlying conditions among all the drive cycles, as the load on the fuel

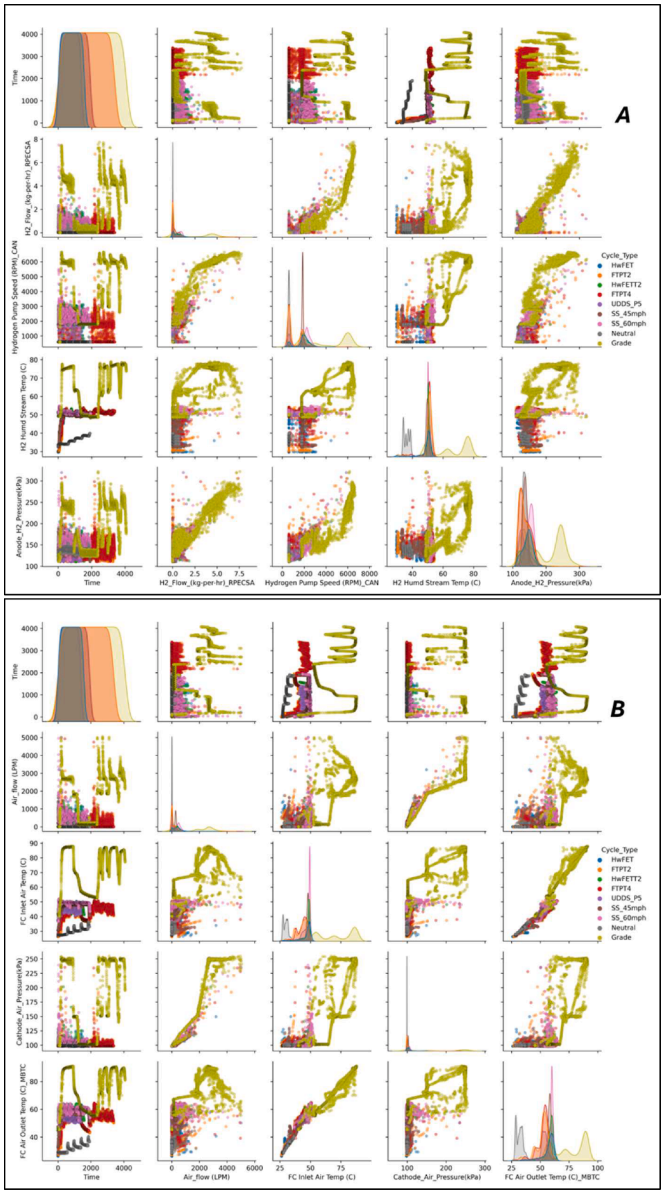

Fig. 4. The reactant attributes of the 2021 Toyota Mirai 2 fuel cell electric vehicle under various loading conditions, as represented by the data acquired in this study: (A) Anode; (B) Cathode.

cell is extremely low or high; this is reflected in the reactant and coolant flow rates being excessively high during the gradient cycle and the coolant temperature being very low during the idle (neutral) condition.

Fig. 4 illustrates the fuel cell stack's reactant flow attributes over different drive cycles. Similar to the electrical and thermal parameters, the gradient cycle stands out with respect to the reactant flow rates and pressures. The anode (H_2) and cathode (air) reactant input follow stoichiometric correlation and exhibit transient behavior over the standard drive cycles.

The bulk of the fuel cell stack's reactant and vehicle data is acquired through CAN, and one of the most taxing problems is signal noise, as the CAN bus operates in an electrically noisy environment, often leading to some signal interference. Despite the precautions to minimize electrical

Table 2
Feature vectors and prediction variables adopted in the present study.

Feature vectors (model inputs)		*Prediction variables (outputs)*
Vehicle-speed	FC H_2 flow	FC avg min voltage
FC stack current	H_2 pump speed	FC stack coolant out T
FC stack coolant in T	H_2 humidity stream temp	FC air outlet T
FC stack coolant flow	H_2 post injector pressure	LIB voltage
FC stack air in T	LIB current	LIB battery temp
FC stack air in P	LIB SOC	
FC air flow	LIB intake air T	
LIB coolant in temp		

interference, some measurement noise is still present in acquiring the vehicle data in real-time during a chassis dynamometer test. It is thus challenging to use vehicle-level data to build advanced machine-learning algorithms to predict system dynamics by implementing data augmentation and signal-conditioning techniques. However, data such as system temperatures, reactant flow rates, and electrical attributes acquired through stand-alone data acquisition systems are relatively robust. As observed from the plots, the hybrid powertrain predominantly operates at the lower end of the spectrum when evaluated on standard drive cycles, and the gradient cycle helps us to capture the reactant flow data on the higher extremes. The pair plots illustrate that the data clusters and parameter correlations aid in understanding the system's nonlinearity; it can be concluded that the data acquired through vehicle testing covers most of the operating conditions for the fuel cell-lithium-ion battery hybrid power system.

4. Machine learning models/data-based modeling

Machine learning techniques are a subset of artificial intelligence that helps develop algorithms that learn and make predictions based on data by recognizing patterns and correlations embedded in the data. These algorithms are adopted in many industries, particularly in sectors or applications that do not have well-defined governing equations or where the process is too complex for mathematical representation and solution. Supervised machine learning involves training a model on a defined dataset acquired from the system, where the input data is paired with the output data during the training process, allowing the model to learn the relationship between inputs and outputs of the system once the training is complete, the developed algorithm mimics the behavior of the system that is trained on.

Supervised machine learning, such as an artificial neural network, is particularly effective for regression prediction problems and is especially suited for multi-input - multi-output (MIMO) systems. Although there are different types of neural network architectures that can be considered for adoption, after analyzing the measurement noise and nonlinearity of the FCEV hybrid system parameters, a simple feed-forward neural network is considered for this study due to its robustness to noise compared to some time series networks. The structural schematic and working of a feed-forward neural network is available in literature [22,33,34,35].

4.1. Feature vector and prediction variable selection

Accurately predicting the fuel cell voltage during various driving conditions purely with a physics-based model is a challenge from a vehicle point of view, and it is critical to understand the difference between the degradation profile and system fault. Similarly, predicting the thermal attributes, such as the fuel cell stack's coolant and air-out

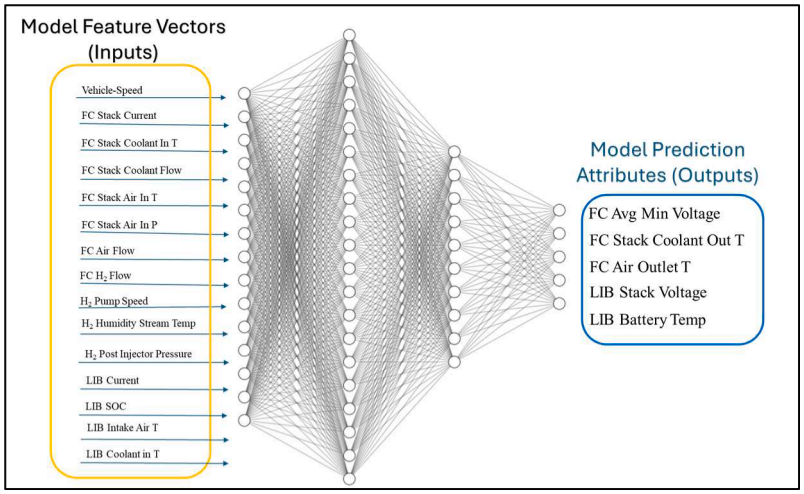

Fig. 5. Schematic of the input, output and architecture of the neural network adopted in the present study.

Table 3
Neural network hyperparameters optimized for the present study.

ANN hyperparameters	*Final value*
Feature vectors (inputs)	15
Target variables (outputs)	5
Number of hidden layers	2
Number of neurons for hidden layers	250 – 1st layer, 150 - 2nd layer
Activation function	'ReLU' – 1, 2 Hidden layers
Loss function	Mean square error - 'MSE'
Optimizer	Adam (learning rate – 0.005, beta_1 = 0.975)
Number of data points	21,146 (Split: 70-training/30 validation)
Batch learning	50
Dropout probability for hidden layers	0.5 – 1st layer, 0.5 - 2nd layer
Loss function	MSE – mean squared error

temperatures, is necessary to identify the formation of hot spots and system health before a catastrophic failure. Precise prediction of battery pack voltage and temperature not only helps from an energy management standpoint but also aids in identifying sensor faults and enhances the system's overall safety.

Because of the reasons mentioned above, fuel cell voltage, coolant out temperature, air outlet temperature, battery pack voltage, and battery temperature are selected as the five prediction variables (model outputs). Considering the fundamental electrochemical governing equations of fuel cells and batteries and the heat transfer basics of thermal management systems, the following feature vectors (model inputs) specified in Table 2 are selected.

4.2. Neural network architecture and hyperparameter tuning

Determining the architecture and hyperparameter for a neural network to mimic the system is the most critical step in model development. Understanding the parameter correlation and nonlinearity of the system is necessary to select the activation function, hidden layers,

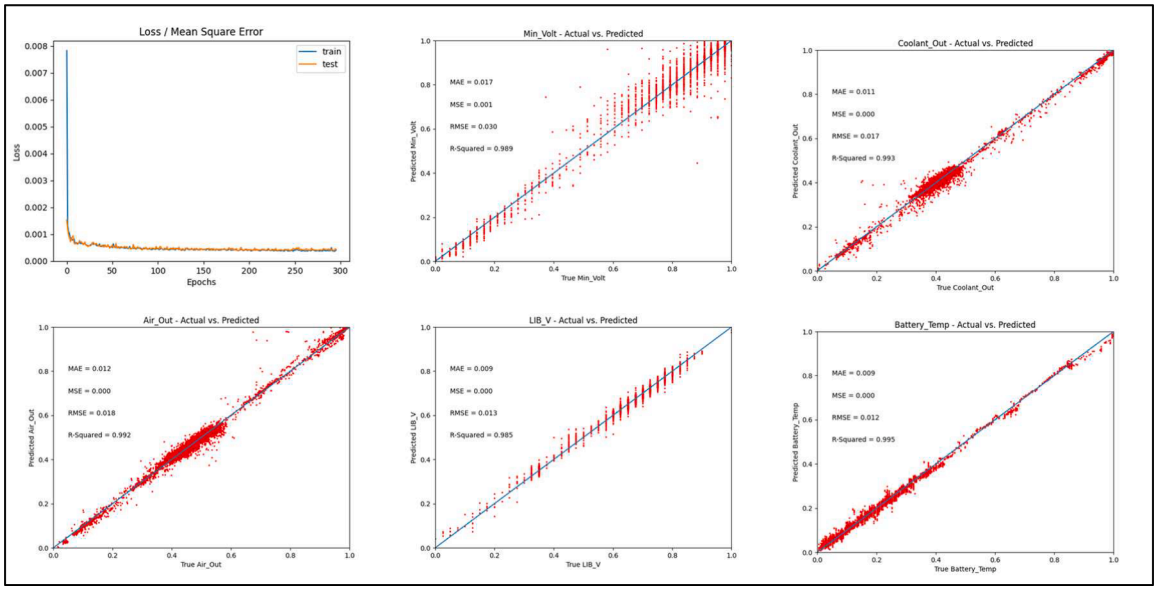

Fig. 6. Prediction accuracy of the trained neural network for various hybrid system attributes.

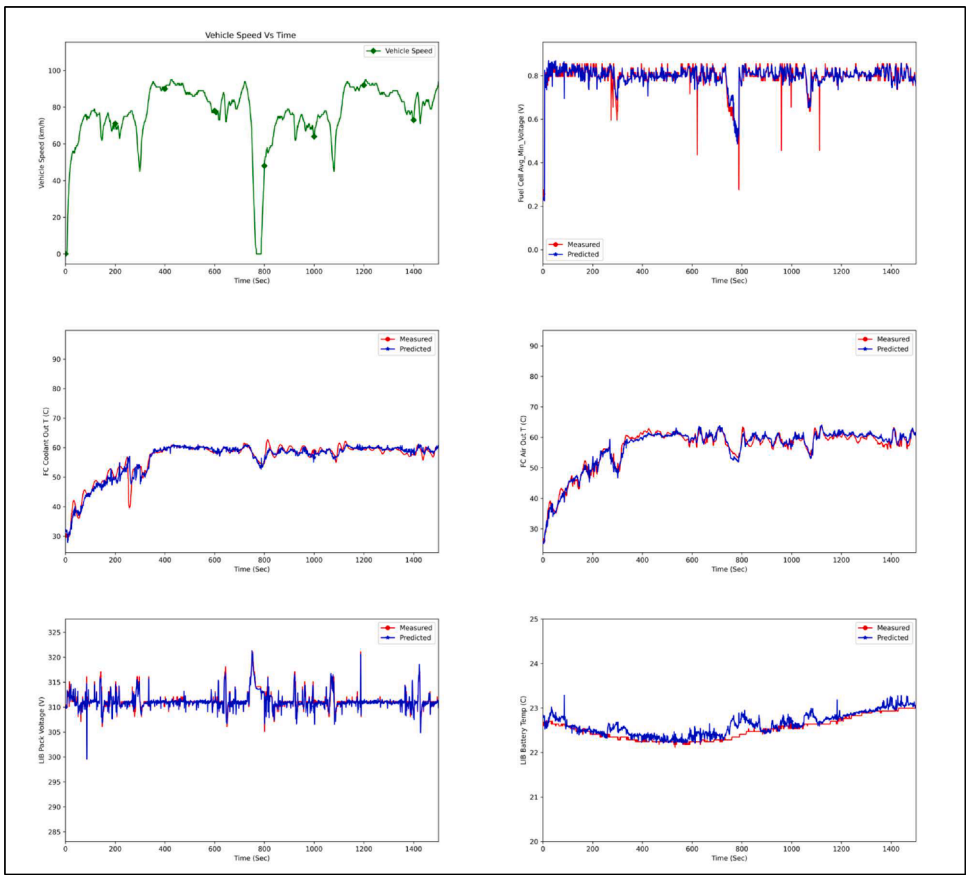

Fig. 7. The performance of the present neural network model for the vehicle operating on HwFET (highway fuel economy test) cycle.

and number of neurons. Considering the computational resources, shallow neural network architecture (two hidden layers) is preferred for automotive applications as deep neural networks require greater storage and higher computational power. A non-exponential activation function, the Rectified Linear Unit (ReLU), is chosen due to its computational efficiency, nonlinearity, sparsity, and relatively quick convergence during training. Optimizing neural network architecture and hyperparameters involves combining domain knowledge and systematic experimentation.

Considering the noise in the CAN data and the system's nonlinearity, a feed-forward neural network is chosen, as described earlier. In contrast, advanced time series-dependent neural network architectures may not yield any significant improvements and sometimes even lead to higher errors in prediction attributes when the data is noisy. The Savitzky-Golay filter [36] is tried with various observation windows and polynomials to smoothen the data without distorting the fundamental behavior of the attribute. Early stopping feature is implemented to limit the epochs, prevent overfitting, and reduce training time. Any extreme outlier data points and noisy data attributes during the data acquisition process are omitted from the data set to prevent any bias or misleading patterns. The feed-forward neural network architecture developed is illustrated in Fig. 5 and the tuned hyperparameters for the network are tabulated in Table 3.

After tuning the neural network with the hyperparameters as given above, the prediction results after normalization are illustrated in Fig. 6; here, the model can predict the output attributes with an accuracy of R-squared value greater than 0.98. In Fig. 6 the points line up on the diagonal when the prediction and experimental values match, and the presence of the scattered points away from the diagonal suggests that some predictions are less accurate, which can be attributed to both noise in the dataset and the limitations of the model. There is a more significant spread of points at higher values, which might suggest that the data's noise or variability increases with the values' magnitude; however, it should be noted that the model should not be predicting the system noise as it indicates the overfitting of the model. In this case, the initial observation of the loss plot shows that training and testing losses are low and stable, suggesting that the model has effectively learned the patterns in the data without overfitting, making the model reliable for these regression tasks.

5. Results and discussion

This section evaluates the performance of the trained model in the prediction of the dynamic characteristics of the Mirai's fuel cell-battery hybrid power system operating under various drive cycles. Once the iteration results during the training are satisfactory, the input data from HwFET, FTP, and Gradient drive cycles are fed into the model as a time series (sequential) to assess the accuracy and the capability of the model developed.

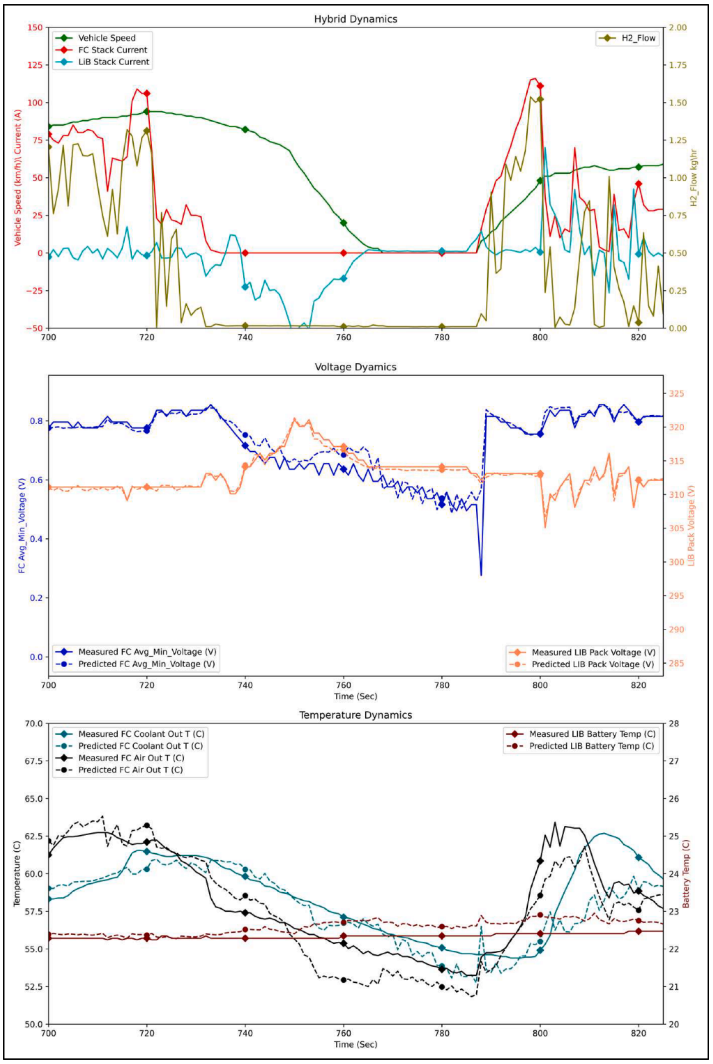

Fig. 8. The fuel cell-battery hybrid power system dynamics and the prediction accuracy of the developed neural network model during a vehicle deceleration and acceleration event for the vehicle operating on the HwFET (highway fuel economy test) cycle.

5.1. *HwFET cycle (highway fuel economy test)*

The HwFET cycle simulates the usual highway driving conditions, which is relatively stable compared to the FTP or Gradient cycle. The average speed is around 77.7 km/h, and the maximum speed reached during the test is approximately 97 km/h (60 mph), including the acceleration and deceleration phases to mimic real-world driving. The vehicle's operating parameters during the HwFET cycle are the model's input to predict the hybrid power system dynamics. The predicted values from the trained model compared to measurement are illustrated in Fig. 7, from which it can be concluded that the model performance during the near steady-state or limited transient conditions is excellent. The model could predict minor changes in the system outputs but does not follow the system noise, demonstrating its robustness.

As it is seen from the vehicle speed subplot shown in Fig. 8, the Mirai vehicle during HwFET is subjected to a hard deceleration and subsequent acceleration event that occurred around 800 s. During this deceleration, the vehicle speed was dropped to zero and accelerated to 60 km/hr; in this instance, a rapid change is observed in the fuel cell-battery hybrid dynamics where the average minimal fuel cell voltage falls below 0.6 V when the vehicle approached idle as both the hydrogen flow and fuel cell stack current drops to zero. On the other hand, LiB stack voltage spikes during deceleration because of the battery regeneration, which can be inferred from the negative LiB stack current. In both cases at the same deceleration instance, the model accurately predicts the drop in fuel cell voltage and increase in battery voltage during the deceleration by correlating the change in vehicle speed, hydrogen fuel flow, fuel cell, and battery current. Similarly, as the vehicle is accelerated, the fuel cell recovers or reverts back to the standard operating voltage of 0.8 V as the hydrogen flow is turned back on proportionally to the vehicle speed, and the LiB stack voltage falls back as the battery stack current is utilized for the vehicle acceleration. The temperature dynamics are relatively unchanged in the HwFET cycle, and the model could accommodate these minor changes by tracking these subtle changes. These results demonstrate the capability of the model to accurately predict the hybrid system dynamics by

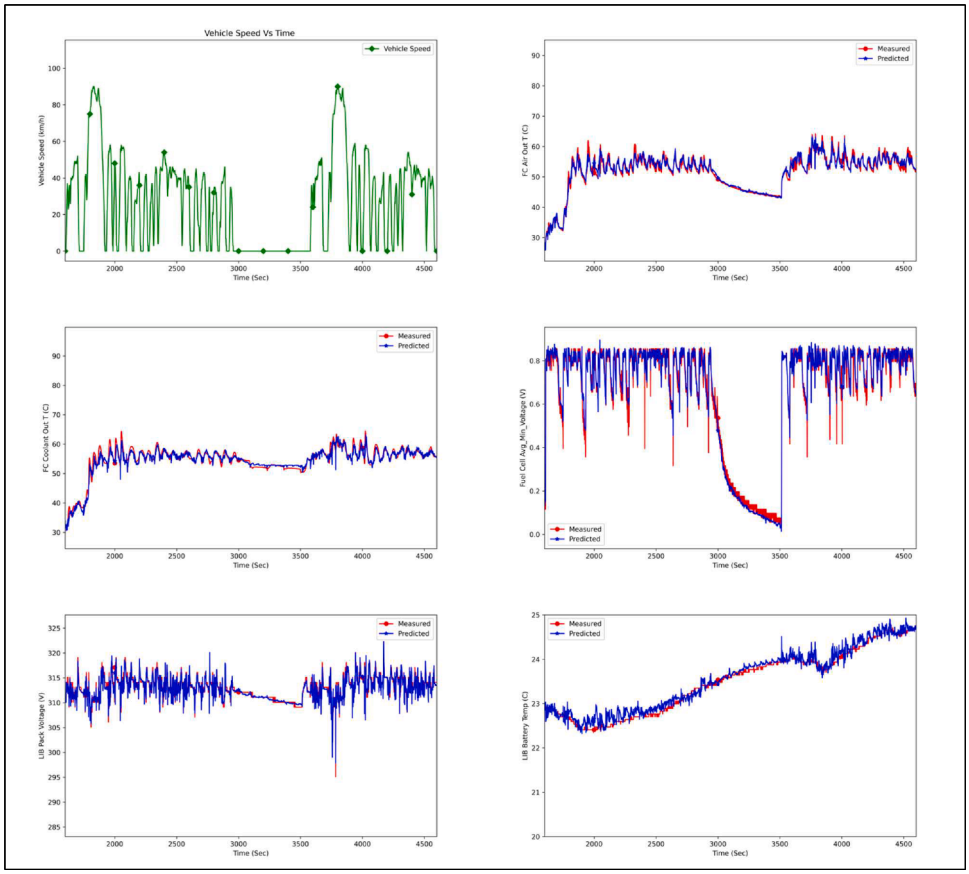

Fig. 9. The performance of the present neural network model for the vehicle operating on the FTP (federal test procedure) cycle.

correlating the vehicle's operational parameters in a near-steady state condition and during challenging decelerate-accelerate events.

5.2. FTP cycle (federal test procedure)

The FTP cycle is a standardized driving test to evaluate emissions and overall performance of a vehicle operating under various driving conditions, which is a relatively more transient drive cycle when compared to HwFET presented earlier. The average speed throughout the cycle is around 34.1 km/h, and the maximum speed reached during the test is approximately 91.2 km/h, including a mix of idling, acceleration, deceleration, and cruising phases to simulate real-world urban and suburban driving conditions. Like the case for HwFET, the operating parameters of the vehicle during the FTP cycle are used as inputs for the model to predict the hybrid power system dynamics during the transient operation. The prediction performance of the trained model is illustrated in Fig. 9. It is evident that the model prediction accuracy in extreme transient conditions is outstanding, especially when compared to similar physics-based models [37,38]. To a certain extent, the model can also distinguish the system noise in extreme transient conditions.

The extreme transient part of the FTP cycle is illustrated in Fig. 10, where the vehicle is subjected to high-frequency acceleration and deceleration events in a short period. As observed from the first minute of the illustrated time series (between 3500 and 3550 s), despite the vehicle being idle, the measured fuel cell voltage is at 0.8 V, the fuel cell stack current is around 20 A, and hydrogen flow fluctuates around 0.5 kg/hr while the measured LiB stack current is around -20A and rising LiB voltage indicates that the fuel cell is recharging the battery as determined by the supervisory controller. Here, the neural network model accurately identifies the battery regeneration event at idle during the start of the second FTP cycle and not only accurately predicts the fuel cell and battery pack voltage simultaneously, but also captures the rising temperature dynamics accurately. On the other hand, there are two more instances between 3560 and 3750 s where the vehicle is idle, and there is no battery regeneration; here, the model accurately distinguishes and predicts the voltage dynamics similarly.

In the second (3600–3700 s) and third phase (3700–3800 s) of the drive cycle, the high-frequency vehicle acceleration-deceleration events pushes the hybrid dynamics into another zone where the bulk of the transient power demand is fulfilled by the fuel cell, and the battery pack supplements and regenerates during the peak transient conditions. Here, the model again accurately correlates the changing transients of the vehicle speed and operating parameters, such as hydrogen flow rate and current outputs, to predict the voltage and temperature dynamics without any time delay (lag) associated with the reactant transport and diffusion dynamics, demonstrating the potential of the developed model for real-time application.

5.3. Gradient cycle

The gradient cycle is a non-standard in-house drive cycle developed to subject the vehicle to high loads and speeds, extracting the rated power to understand the powertrain system behavior at extreme conditions, as typical automotive drive cycles do not cover the entire

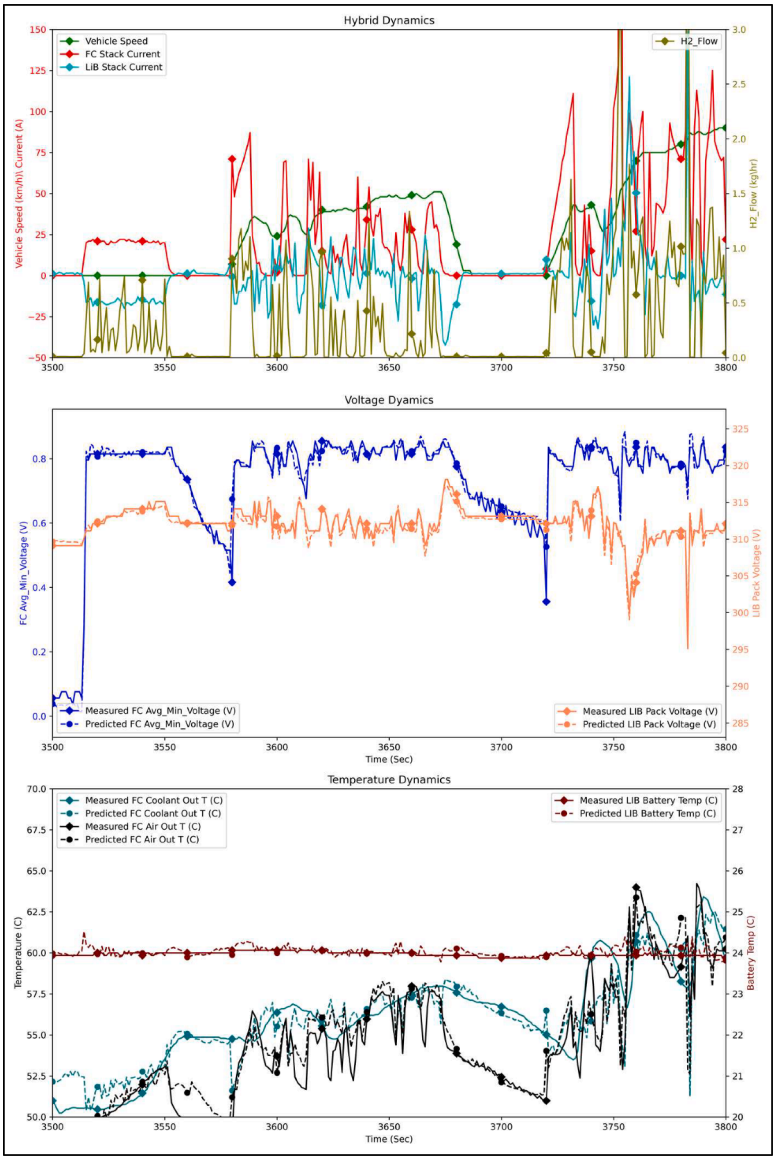

Fig. 10. The hybrid power system dynamics and the prediction accuracy of the developed neural network model during high-frequency deceleration and acceleration events for the vehicle operating on the FTP (federal test procedure) cycle.

operating spectrum of the vehicle. Gradient cycle pushes the system performance to its design limits, as in this case, the vehicle hits the thermal derate to protect the fuel cell system from being exposed to excessive high operating temperatures. This cycle combines idle, steady-state, and transient modes where the operating parameters of the vehicle are fed as inputs to the model for the prediction of the powertrain system output attributes in extreme conditions. The measured and predicted results are illustrated in Fig. 11, where a wide range of fluctuations in the system attributes, such as rising system temperatures and dropping voltages during acceleration, can be observed. Fig. 11 shows that the model prediction is in good agreement with the experimental data, encompassing the entire fuel cell hybrid operational spectrum, even for extreme conditions.

Fig. 12 illustrates the final phase, or the most challenging part of the gradient cycle, where the vehicle is subjected to transient driving conditions almost at rated power. In the first half of the illustrated timer series (between 20,500 and 20,800 s), the vehicle is subjected to quick deceleration followed by rapid acceleration at a high load in the second phase (after 20,800 s). As observed from Fig. 12, the vehicle is operated in extreme conditions at almost thrice the hydrogen fuel flow rate and fuel cell stack current with fuel cell temperature dynamics consistently over 85°C to reach a vehicle speed close to 120 km/hr. Here, the neural network model identifies both the deceleration and acceleration events under these extreme operating conditions and accurately predicts the wide swings in the fuel cell and battery voltages along with temperature dynamics.

The rapid change in the fuel cell temperature dynamics can be observed at the end of the deceleration and the start of the acceleration phase (20,600–20,900 s), where both the fuel cell coolant out and air (cathode) outlet temperatures fall and rise between 65 C and 95 C coupled with the swings in fuel cell voltage and LiB stack voltage. Here, the model correlates the extreme operating conditions and predicts the

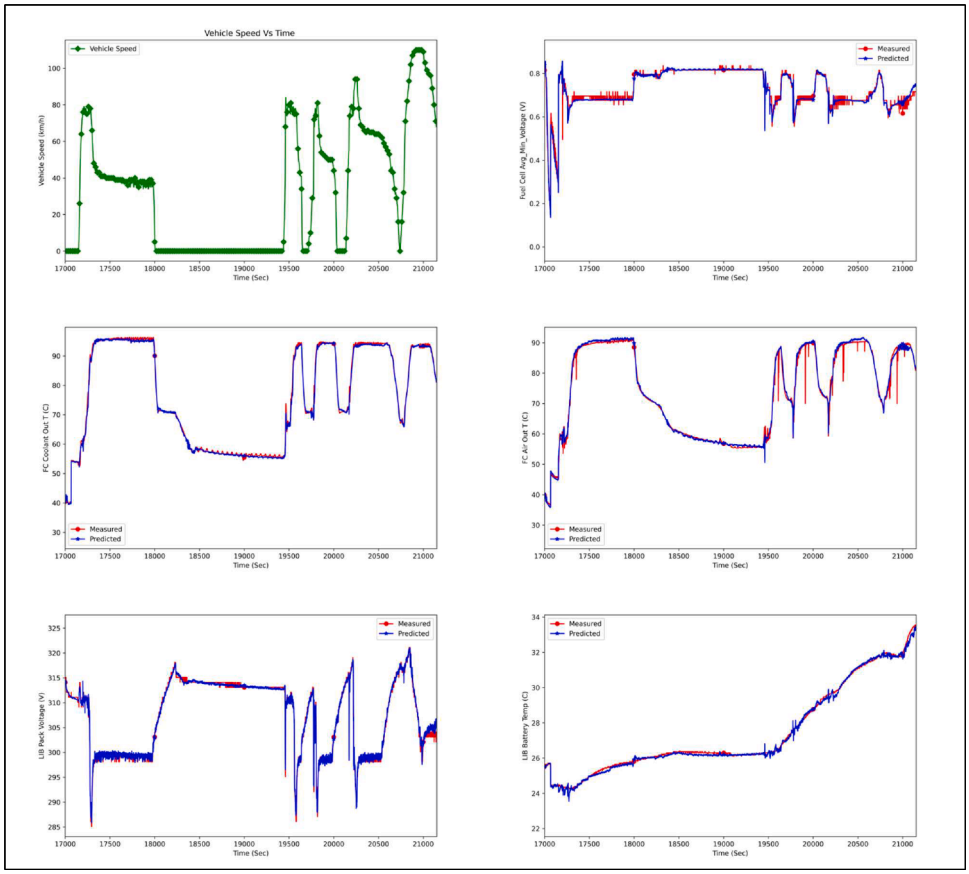

Fig. 11. The performance of the present neural network model for the vehicle operating on the gradient cycle.

fluctuations in temperatures and voltages across all the transient phases without any significant changes in the prediction accuracy and also avoids replicating the measurement noise to some extent, demonstrating the robustness and applicability of such models across broad operating spectrums.

It is crucial to consider a range of error metrics that provide a more comprehensive assessment of the model's prediction accuracy. Metrics like Mean Absolute Error (MAE), Mean Squared Error (MSE), Root Mean Squared Error (RMSE), and Mean Absolute Percentage Error (MAPE) offer valuable insights into different aspects of prediction accuracy. MAE provides a straightforward measure of average absolute errors, MSE emphasizes more significant errors due to its squaring nature, RMSE offers a measure of error magnitude that is interpretable in the same units as the original data, and MAPE gives an understanding of the average error as a percentage of the actual values. By considering these metrics together, as shown in Table 4, a more nuanced and complete evaluation of a model's performance can be achieved, especially in the context of complex, nonlinear, or transient data.

The above results suggest that the presently trained machine-learning model has accurately predicted the Mirai vehicle's critical fuel cell hybrid power system attributes, even under extreme transient operating conditions with noisy measurement and limited signal processing. The computational speed for each time step is around 740 Microseconds, or ~ 0.00074 s when operated on a computer equipped with an Nvidia Graphic Card – RTX 3070, 12th Gen Intel (R) Core (TM) i9-12900, and 32 GB of RAM. Considering the model development time, computational speed, and excellent prediction performance, the developed machine learning model has great potential for use in diagnostics and product development.

6. Conclusions

In this study, a full-fledged machine-learning model based on a feed-forward neural network has been developed to model the dynamics of the fuel cell-lithium-ion battery (LIB) hybrid power system implemented in the 2021 Toyota Mirai 2nd generation fuel cell electric vehicle. The data is acquired from the vehicle in real-time during a chassis dynamometer test under various driving cycles, including the US Environmental Protection Agency's Urban Dynamometer Driving Schedule (UDDS) and the Highway Fuel Economy Driving Schedule (HFEDS), Federal Test Procedure (FTP), Highway Fuel Economy Test (HwFET), Neutral Cycle, and Grade Testing Cycle. During the training and validation phase, the model utilizes the data generated from the vehicle's onboard controller area network (CAN) bus and other data acquisition systems. Over 21,000 data points across the different driving cycles are acquired from the vehicle testing to understand the dynamic characteristics and nonlinearity of the fuel cell battery hybrid powertrain system under the various operating conditions. After analysis, 15 operating parameters are chosen as the feature vectors for the neural network mode to predict the average minimum cell voltage, coolant, and cathode out air outlet temperatures of the fuel cell, along with LiB voltage and temperature. The hyperparameters used for training the neural network, testing cases, and resultant data spread are analyzed, and the trained model demonstrates excellent accuracy in predicting the fuel cell-battery hybrid power system dynamics with an accuracy of R-squared value greater than 0.98. The neural network model performance across the various drive cycles representing steady state and extreme transient operating conditions is outstanding and robust despite measurement noise, illustrating their applicability in system development and onboard diagnostic systems.

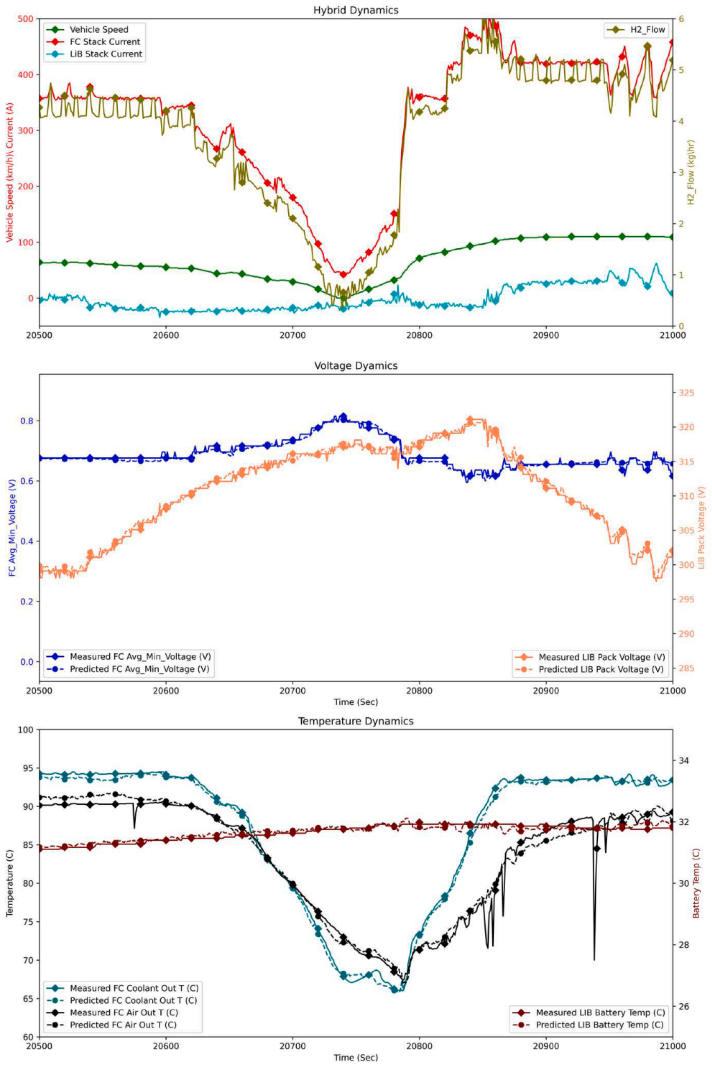

Fig. 12. The hybrid power system dynamics and the prediction accuracy of the present neural network model during extreme driving conditions at the rated power for the vehicle operating on the gradient cycle.

Table 4
Error attributes for the model predicted fuel cell-battery electric-electric hybrid power system attributes over the different drive cycles investigated.

Cycle	*Predicted parameter*	*MSE*	*RMSE*	*MAE*	*MAPE*
HwFET	Fuel cell avg_min_voltage (V)	0.001	0.028	0.014	2.17 %
	FC coolant out T (C)	2.802	1.674	1.004	1.92 %
	FC air out T (C)	1.532	1.238	1.001	1.82 %
	LIB pack voltage (V)	0.224	0.473	0.348	0.11 %
	LIB battery temp (C)	0.021	0.146	0.113	0.50 %
FTP	Fuel cell avg_min_voltage (V)	0.001	0.032	0.021	5.06 %
	FC coolant out T (C)	1.617	1.271	0.925	1.70 %
	FC air out T (C)	1.183	1.088	0.799	1.54 %
	LIB pack voltage (V)	0.289	0.537	0.422	0.13 %
	LIB battery temp (C)	0.015	0.122	0.096	0.41 %
Gradient	Fuel cell avg_min_voltage (V)	0.000	0.014	0.009	1.32 %
	FC coolant out T (C)	0.622	0.789	0.545	0.73 %
	FC air out T (C)	1.514	1.230	0.728	1.00 %
	LIB pack voltage (V)	0.361	0.601	0.449	0.15 %
	LIB battery temp (C)	0.018	0.135	0.102	0.37 %

MSE – Mean Squared Error; RMSE – Root Mean Squared Error; MAE – Mean Absolute Error; MAPE – Mean Absolute Percentage Error.

CRediT authorship contribution statement

Adithya Legala: Writing – original draft, Visualization, Validation, Methodology, Investigation, Formal analysis, Data curation, Conceptualization. **Matthew Kubesh:** Visualization, Validation, Methodology, Investigation, Data curation. **Venkata Rajesh Chundru:** Visualization, Validation, Methodology, Investigation, Formal analysis, Data curation. **Graham Conway:** Supervision, Resources, Project administration, Funding acquisition. **Xianguo Li:** Writing – review & editing, Visualization, Validation, Supervision, Resources, Project administration, Methodology, Investigation, Funding acquisition, Formal analysis, Conceptualization.

Declaration of competing interest

The authors declare that they have no known competing financial interests or personal relationships that could have appeared to influence the work reported in this paper.

Acknowledgment

The authors want to specially thank the late Dr. Bapi Raju Surampudi for his strong vision and guidance and acknowledge Southwest Research Institute (SwRI) and senior management of the Powertrain division for providing appropriate resources. We (AL and XL) would also like to acknowledge the partial financial support for this project provided by the Natural Sciences and Engineering Research Council of Canada via a Discovery Grant.

References

[1] IEA. World energy outlook 2016. IEA, Paris 2016. https://www.iea.org/reports/world-energy-outlook-2016. Licence: CC BY 4.0.
[2] Kumar R, et al. Transforming the transportation sector: mitigating greenhouse gas emissions through electric vehicles (EVs) and exploring sustainable pathways. AIP Adv 2024;14(3). https://doi.org/10.1063/5.0193506. Mar.
[3] Liu F, Zhao F, Liu Z, Hao H. The impact of fuel cell vehicle deployment on road transport greenhouse gas emissions: the China case. Int J Hydrogen Energy 2018;43(50):22604–21. https://doi.org/10.1016/j.ijhydene.2018.10.088. Dec.
[4] Bekel K, Pauliuk S. Prospective cost and environmental impact assessment of battery and fuel cell electric vehicles in Germany. Int J Life Cycle Assess 2019;24(12):2220–37. https://doi.org/10.1007/s11367-019-01640-8. Dec.
[5] Li J, et al. Liquid pump-enabled hydrogen refueling system for heavy duty fuel cell vehicles: fuel cell bus refueling demonstration at stark area regional transit authority (SARTA). Int J Hydrogen Energy 2021;46(78):38575–87. https://doi.org/10.1016/j.ijhydene.2021.09.112. Nov.
[6] Maity A, Sarkar S. Data-driven probabilistic energy consumption estimation for battery electric vehicles with model uncertainty. Int J Green Energy 2023. https://doi.org/10.1080/15435075.2023.2276174.
[7] Sun Y, Xia C, Yin B, Gao H, Han J, Liu J. Energy management strategy for FCEV considering degradation of fuel cell. Int J Green Energy 2023;20(1):28–39. https://doi.org/10.1080/15435075.2021.2023546.
[8] Cost, effectiveness, and deployment of fuel economy technologies for light-duty vehicles. National Academies Press; 2015. https://doi.org/10.17226/21744.
[9] Gallo M, Marinelli M. The impact of fuel cell electric freight vehicles on fuel consumption and CO2 emissions: the case of Italy. Sustainability (Switzerland) 2022;14(20). https://doi.org/10.3390/su142013455. Oct.
[10] Yoshizumi T, Kubo H, Okumura M. Development of high-performance FC stack for the new MIRAI. SAE technical papers. SAE International; 2021. https://doi.org/10.4271/2021-01-0740. Apr.
[11] Hasegawa T, Imanishi H, Nada M, Ikogi Y. Development of the fuel cell system in the Mirai FCV. SAE technical papers. SAE International; 2016. https://doi.org/10.4271/2016-01-1185. Apr.
[12] Bartolucci L, et al. Fuel cell hybrid electric vehicles: fuel cell experimental characterization and modeling towards the development of a hardware-in-the-loop platform for advanced powertrain design. J Phys Conf Ser 2023. https://doi.org/10.1088/1742-6596/2648/1/012063. Institute of Physics.
[13] Ryu JH, Lee HJ, Sunwoo MH. An electric powertrain modelling of a fuel cell hybrid electric vehicle and development of a power distribution algorithm using h∞control. In: Proceedings of the institution of mechanical engineers, part d: journal of automobile engineering. Professional Engineering Publishing; 2010. p. 1021–39. https://doi.org/10.1243/09544070JAUTO1269. Aug.
[14] Vichard L, Steiner NY, Zerhouni N, Hissel D. Hybrid fuel cell system degradation modeling methods: a comprehensive review. J Power Sources 2021;506. https://doi.org/10.1016/j.jpowsour.2021.230071. Sep. 15.
[15] Zhao J, Li X, Shum C, McPhee J. A review of physics-based and data-driven models for real-time control of polymer electrolyte membrane fuel cells. Energy and AI 2021;6:100114. https://doi.org/10.1016/j.egyai.2021.100114.
[16] Chan CC, Bouscayrol A, Chen K. Electric, hybrid, and fuel-cell vehicles: architectures and modeling. IEEE Trans Veh Technol 2010;59(2):589–98. https://doi.org/10.1109/TVT.2009.2033605. Feb.
[17] Hasegawa S, Ikogi Y, Kim S, Kageyama M, Kawase M. Modeling of the dynamic behavior of an integrated fuel cell system including fuel cell stack, air system, hydrogen system, and cooling system. ECS Trans 2022;109(9):15–70. https://doi.org/10.1149/10909.0015ecst. Sep.
[18] Mizutani C, Shiozawa M, Maruo T, Aso S. On-board control system of water content inside FCV stack by electrochemical impedance spectroscopy. ECS Trans 2017;80(8):357–65. https://doi.org/10.1149/08008.0357ecst. Aug.
[19] Kulikovsky AA. Analytical modeling of fuel cells. Analytical Modeling of Fuel Cells 2019:1–382. https://doi.org/10.1016/C2018-0-01182-2.
[20] Pukrushpan BJT, Stefanopoulou AG, Peng H. Avoid fuel cell oxygen starvation with air flow controllers. IEEE Contr Syst Mag 2004;(April):30–46.
[21] J.T. Pukrushpan and Jay Tawee Pukrushpan, "Modeling and control of fuel cell systems and fuel processors," 2003. [Online]. Available: http://www-personal.umich.edu/~annastef/FuelCellPdf/pukrushpan_thesis.pdf.
[22] Legala A, Shahgaldi S, Li X. Data-based modelling of proton exchange membrane fuel cell performance and degradation dynamics. Energy Convers Manag 2023;296:117668. https://doi.org/10.1016/j.enconman.2023.117668. Nov.
[23] J. Zhao, "Catalyst layers in polymer electrolyte membrane fuel cells: formation, characterization and performance," 2019, [Online]. Available: https://uwspace.uwaterloo.ca/handle/10012/14425.
[24] Zhao J, Li X. A review of polymer electrolyte membrane fuel cell durability for vehicular applications: degradation modes and experimental techniques. Energy Convers Manag 2019;199(September 2019):112022. https://doi.org/10.1016/j.enconman.2019.112022.
[25] Shahgaldi S, Alaefour I, Zhao J, Li X. Impact of ionomer in the catalyst layers on proton exchange membrane fuel cell performance under different reactant flows and pressures. Fuel 2018;227:35–41. https://doi.org/10.1016/j.fuel.2018.04.076. Sep.
[26] Carignano M, Costa-Castelló R. Toyota Mirai: powertrain model and assessment of the energy management. IEEE Trans Veh Technol 2023;72(6):7000–10. https://doi.org/10.1109/TVT.2023.3237173. June.
[27] KoteswaraRao.K V, Naga Srinivasulu G. Modeling, downsizing, and performance comparison of a fuel cell hybrid mid-size car with FCEV for urban and hill road driving cycles. Int J Green Energy 2019;16(2):115–24. https://doi.org/10.1080/15435075.2018.1549996. Jan.
[28] M. Meindl, R. Oechsner, M. Maerz, M. März, R. Öchsner, and J. Geiling, "Reverse engineering of the hydrogen system of a commercial fuel cell vehicle CO2 pump laser development for FIR lasers view project thermal management solutions for complex battery systems view project reverse engineering of the hydrogen system of a commercial fuel cell vehicle," 2023. [Online]. Available: https://orcid.org/0000-0002-4808-1749.
[29] Maruo T, et al. Development of fuel cell system control for sub-zero ambient conditions. SAE technical papers. SAE International; 2017. https://doi.org/10.4271/2017-01-1189. Mar.
[30] SAE international recommended practice, chassis dynamometer simulation of road load using coastdown techniques. SAE Standard J2264_202301 2023. https://doi.org/10.4271/J2264_202301. Revised JanuaryIssued April 1995.
[31] SAE International Recommended Practice. Recommended practice for measuring fuel consumption and range of fuel cell and hybrid fuel cell vehicles fueled by compressed gaseous hydrogen. SAE Standard J2572_201410 2014. https://doi.org/10.4271/J2572_201410. Revised OctoberIssued August 2006.
[32] Dynamometer drive schedules | US EPA. US EPA 2024. 17 May, www.epa.gov/vehicle-and-fuel-emissions-testing/dynamometer-drive-schedules.
[33] Legala A, Zhao J, Li X. Machine learning modeling for proton exchange membrane fuel cell performance. Energy and AI 2022;10:100183. https://doi.org/10.1016/j.egyai.2022.100183. Nov.
[34] Caponetto R, Guarnera N, Matera F, Privitera E, Xibilia MG. Application of electrochemical impedance spectroscopy for prediction of fuel cell degradation by LSTM neural networks. In: 2021 29th mediterranean conference on control and automation, MED 2021. Institute of Electrical and Electronics Engineers Inc.; 2021. p. 1064–9. https://doi.org/10.1109/MED51440.2021.9480253. Jun.
[35] Legala A, LakkiReddy V, Weber P, Li X. Modeling of diesel particulate filter temperature dynamics during exotherm using neural networks. Front Therm Eng 2023;3. https://doi.org/10.3389/fther.2023.1265490. Oct.
[36] Jiao M, Wang D. The Savitzky-Golay filter based bidirectional long short-term memory network for SOC estimation. Int J Energy Res 2021;45(13):19467–80. https://doi.org/10.1002/er.7055. Oct.
[37] He W, et al. A novel high-dimensional and multi-physics modeling approach of proton exchange membrane fuel cell for real-time simulation. Energy Convers Manag 2023;286. https://doi.org/10.1016/j.enconman.2023.116988. Jun.
[38] Ritzberger D, Hametner C, Jakubek S. A real-time dynamic fuel cell system simulation for model-based diagnostics and control: validation on real driving data. Energies (Basel) 2020;13(12). https://doi.org/10.3390/en13123148. Jun.